

Isolation of the Zenneck Surface Wave

Janice Hendry

Roke Manor Research Limited
Romsey, UK

janice.hendry@roke.co.uk

Abstract— This paper focuses on the methodology and results regarding the isolation of the Zenneck surface wave using finite element simulation techniques. An idealised surface to provide an optimal surface for Zenneck surface wave propagation. By comparing the unique theoretical properties of the Zenneck surface wave to the results of these simulations it was found that the simulations did exhibit characteristics of a Zenneck surface wave.

I. INTRODUCTION

There are several variants of surface waves, however only the Zenneck surface wave is considered in this paper and therefore all future references to surface waves herein will relate to the Zenneck type.

Creeping waves are often confused with surface waves although they are two distinct phenomena. A surface wave can be defined as “a wave that propagates along an interface between two media without radiation” [1].

A creeping wave should be differentiated as they can be described by the geometrical theory of diffraction [3], i.e. it represents a diffracted wave travelling around an object. On a perfectly electrically conducting (PEC) sphere, for example, diffracted waves do appear to ‘creep’ around the metallic structure mimicking the surface-following behaviour of surface waves. However creeping waves radiate as they travel around the surface and so cannot be considered a true surface wave.

A Zenneck surface wave, in contrast, is a transverse magnetic (TM), inhomogeneous plane wave that is bound to an interface and is non-radiating.

This work has been investigating the possibility of using the Zenneck surface wave to propagate over the Earth’s surface. This paper focuses specifically at isolating the Zenneck surface wave in simulation software with the aim of extrapolating this to a non-idealised environment.

II. SURFACE WAVE PROPAGATION

A. Boundary Conditions

To obtain a solution to Maxwell’s equations for a plane Zenneck surface wave, the following assumptions can be made (see Figure 3):

- no field variation in the y -direction (plane wave condition). Therefore, $\partial/\partial y=0$;
- field variations in the x -direction can be represented by $\exp(-\gamma_0 x)$ in the dielectric and by $\exp(-\gamma_1 x)$ in the medium;
- field variations in the z -direction are as yet unknown and must be solved for.

where x is the direction of propagation and z is in a direction vertically away from the boundary.

When these conditions are applied to Maxwell’s equations the following solutions outside the medium [1], with the time-dependent factor omitted, are:

$$H_y = A \exp(-uz) \exp(-\gamma x) \quad (1)$$

$$E_x = -\left(\frac{u}{\sigma + j\omega\epsilon}\right) A \exp(-uz) \exp(-\gamma x) \quad (2)$$

$$E_z = \left(\frac{\gamma}{\sigma + j\omega\epsilon}\right) A \exp(-uz) \exp(-\gamma x) \quad (3)$$

where,

$$k^2 = -j\omega\mu(\sigma + j\omega\epsilon) \quad (4)$$

$$\gamma = \alpha + j\beta \quad (5)$$

$$u^2 = -(k^2 + \gamma^2) \quad (6)$$

and, σ =conductivity; ω =angular frequency; ϵ =permittivity; μ =permeability; k =intrinsic propagation coefficient for the propagation medium below the interface (4); γ =propagation coefficient along interface (5).

In order to satisfy Maxwell’s Equations all the field components should be equal at the boundary, $z=0$. This solution is known as the “resonance condition” [2] and when satisfied, is a valid solution to Maxwell’s Equations, with E_x , E_z and H_y field components, supported by a flat surface and characterised by an exponential decay of the field on both sides of the boundary.

If one now considers the radial Zenneck surface wave to obtain the expected decay rate in the direction of propagation the following solutions outside the medium are obtained:

$$H_\phi = A \exp(-uz) H_1(-j\gamma r) \quad (7)$$

$$E_x = A \left(\frac{u}{\sigma + j\omega\epsilon}\right) \exp(-uz) H_1(-j\gamma r) \quad (8)$$

$$E_z = -A \left(\frac{j\gamma}{\sigma + j\omega\epsilon}\right) \exp(-uz) H_0(-j\gamma r) \quad (9)$$

where, H represents the Hankel function. At large radii [1] this approximates to,

$$H_0(-j\gamma r) \approx \sqrt{\frac{2}{j\pi\gamma r}} \exp(-\gamma r) \exp(j\frac{1}{4}\pi) \quad (10)$$

$$H_1(-j\gamma r) \approx \sqrt{\frac{2j}{\pi\gamma r}} \exp(-\gamma r) \exp(j\frac{3}{4}\pi) \quad (11)$$

The above equations therefore show that the E-field decay rate in the direction of propagation is proportional to $\frac{1}{\sqrt{r}}$.

B. Idealised Surface

[1] states that the optimal surface for the propagation of a surface wave is purely reactive. A suitably designed corrugated metallic surface meets this requirement as it has a purely reactive surface impedance.

Consider the corrugated surface shown in Figure 1. The surface impedance is given by:

$$Z_S = jZ_W \left(\frac{d}{D} \right) \tan \left(\frac{2\pi h}{\lambda} \right) \quad (12)$$

where d, D and h are defined in Figure 1, λ is the wavelength and Z_W is the impedance of the material in the grooves, e.g. Z_0 for air (377 Ohms).

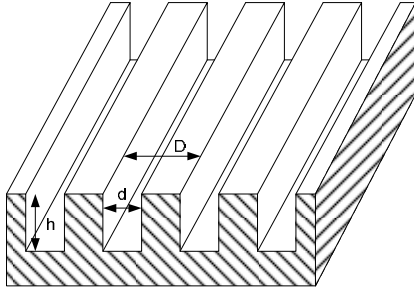


Figure 1 Corrugated Surface

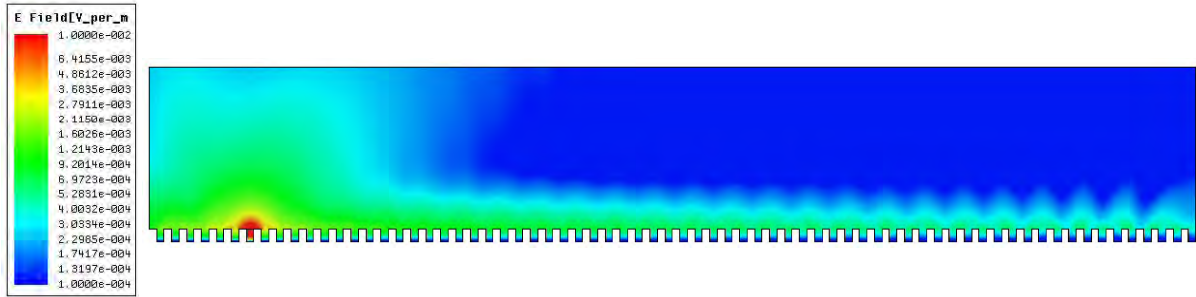


Figure 2 Corrugations Creating an Inductive Reactance: Bound Wave Propagation Visible

III. SIMULATION RESULTS

A. Field Structure

The expected field structure of a surface wave is shown in Figure 3. In order to verify that Figure 2 is actually showing a surface wave, a similar field structure to that shown in Figure 3 should be evident. The E-field vectors were plotted to see if this structure was visible. Figure 4 shows the vector E-field and the expected field structure can be observed which provides good evidence that a surface wave is present. The difference between the fields with the surface wave present (Figure 4) and the surface wave absent (Figure 5) is particularly evident.

A metallic corrugated surface has zero loss, any losses seen will be due to spreading. This knowledge enables the properties of a Zenneck surface wave to be demonstrated in simulation software.

From Equation 12, it can be shown that an inductive surface reactance can be produced if the corrugation depth is less than a quarter wavelength and not less than its width. [1] suggests that for the surface impedance to appear uniform, at least three complete corrugations within a wavelength are required.

C. Simulation Methodology

Ansoft's High Frequency Structure Simulator (HFSS) software was used for all of the simulations detailed in this paper. HFSS is a general purpose finite element electromagnetic simulation tool.

The simulation shown in Figure 2 was run at 1 MHz and was greater than 10 wavelengths in length, however it is expected that this behaviour will scale with frequency.

Using the unique properties of a surface wave and an idealised surface, the simulation results can be analysed to show that a surface wave is present. The following properties were assessed:

1. Field structure;
2. Decay rate away from boundary and from source;
3. Interface acts as waveguide.

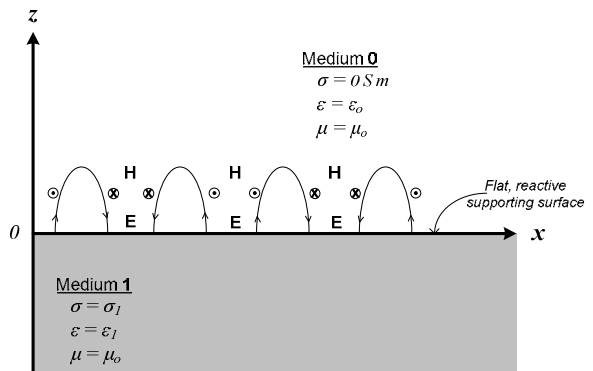


Figure 3 Expected Field of a Zenneck Surface Wave

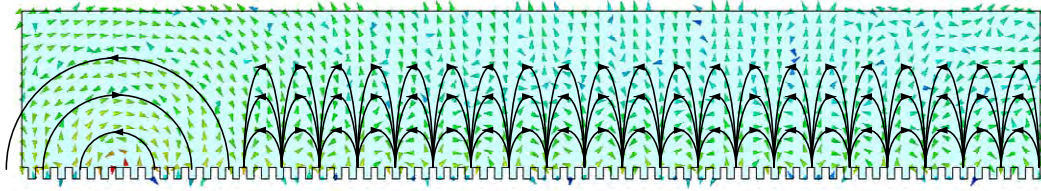


Figure 4 E-field vector plot demonstrating presence of the Zenneck Surface Wave

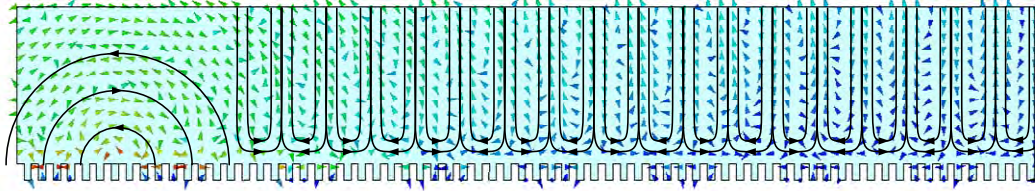


Figure 5 E-field vector plot with no surface wave present

B. Field Decay

E-field cuts were taken to examine how the field decays horizontally from the source along the boundary and vertically away from the boundary (Figure 6). If a surface wave is present, the E-field decay rate from the source horizontally along the boundary should be approximately $\frac{1}{\sqrt{r}}$ (where r is distance from the source) and exponential vertically away from the boundary. The results from the simulation can be plotted and compared to theory. It was assumed that a space wave was the field which appeared not to be bound to the corrugations. Some space wave will be present as the source used was not a perfect surface wave launcher. In order to excite a perfect, fully bound surface wave, [1] states that a launcher with infinite aperture perpendicular to the boundary is required in addition to an ideal surface.

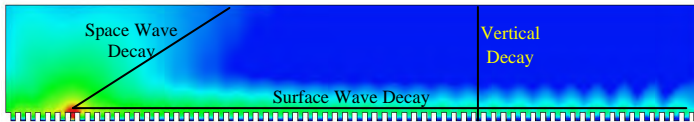


Figure 6 Field Cuts to Examine E-field Decay Rate

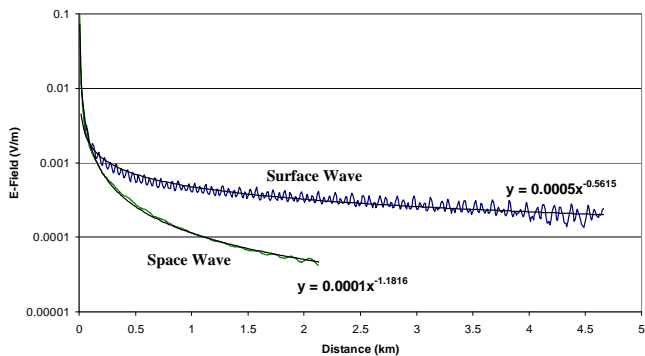


Figure 7 Decay Rate Away From Source

In Figure 7, the E-field along the line marked 'Space Wave' decays away at $r^{-1.18} \approx \frac{1}{r}$ based on the line of best fit. It is not exactly $\frac{1}{r}$ due to limitations in the simulation

software. However, this decay rate contrasts dramatically with the E-field along the line marked 'Surface Wave' where the E-field decays at $r^{-0.56} \approx \frac{1}{\sqrt{r}}$. The ripple in the

raw data from the simulation is due to slight variations in the field caused by the corrugated surface and reflections from the boundaries/end of the corrugations due to limitations in the simulation software.

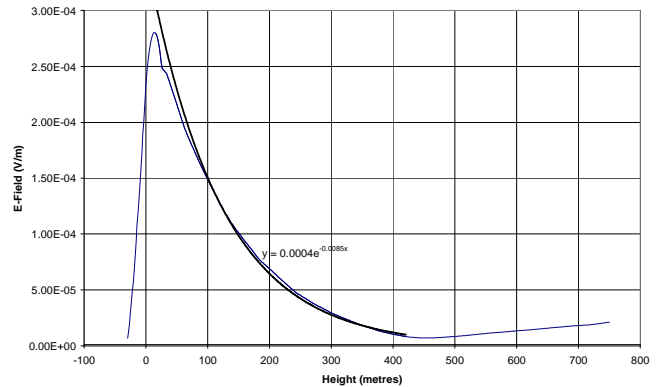


Figure 8 Decay Rate Away from Boundary

In Figure 8 the E-field increases from the bottom of the trough and reaches a peak just above the surface of the corrugations. The field then decreases exponentially with respect to distance up to about 450 metres. This exponential decay rate shows excellent agreement with surface wave theory for the chosen frequency and surface configuration and is further evidence that a surface wave is being simulated. Above 450 metres the field increases again which is most likely where the space wave becomes dominant.

C. Bound Wave

To show that the interface is acting as a waveguide and that the wave is therefore bound to the surface a gradient was introduced in the simulation. It is possible to define the surface impedance of a surface in HFSS without needing to simulate the complexity of corrugations. It can be seen in Figure 9 that if a suitably reactive surface ($10+j300$ Ohms

surface impedance) is chosen the wave will remain bound even if a 45 degree gradient is introduced. Once again, a space wave is present as the source is not perfect. Additionally, due to limitations in the simulation software, a resistance must be included (loss mechanism) for convergence.

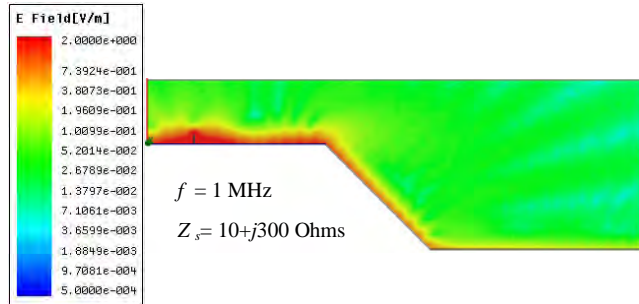


Figure 9 Bound Wave Over a 45 degree Gradient for an Inductive Reactive Surface

To confirm that this is due to the wave being bound, it can be compared to a PEC surface where no surface wave should be present (Figure 10).

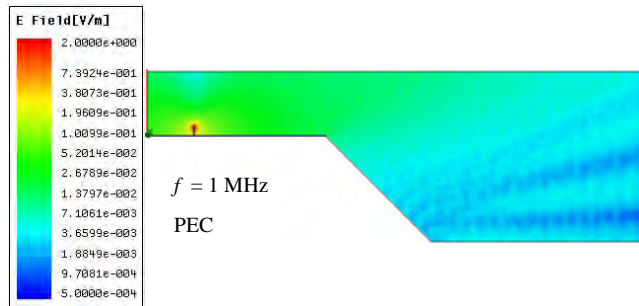


Figure 10 No Bound Wave Present Over a 45 degree Gradient for PEC Surface

It can easily be seen when comparing the above two simulation results that the wave is being guided by the reactive surface. Some field is still present after the gradient in the PEC simulations; however this is due to diffraction.

IV. CONCLUSIONS

By using an idealised surface, it has been possible to demonstrate the Zenneck surface wave in HFSS. This has been verified by comparing some of the unique properties of the Zenneck surface wave with simulation results and this paper has shown there is a good correlation with theory and thus it is indicative that a surface wave is present in these simulations and this technique can now be extended for use on non-idealised surfaces.

ACKNOWLEDGEMENTS

The author would like to acknowledge Mike Jessup's invaluable assistance through-out this work

The work reported in this paper was funded by the Systems Engineering for Autonomous Systems (SEAS) Defence Technology Centre (DTC) established by the UK Ministry of Defence.

This work will form part of an Engineering Doctorate (EngD) at UCL, with fees funded by the EPSRC.

REFERENCES

- [1] H. Barlow, J. Brown, *Radio Surface Waves*, Oxford University Press, London (1962)
- [2] J. Wait, *Electromagnetic Waves in Stratified Media*, IEEE Press, IEEE/OUP Reissue, USA, 1996
- [3] W. Franz, *Z. Naturforsch., Über die greensche funktionen des zylinders und der kugel*, 9a, pp. 705-716, 1954
- [4] J. Hendry, *Factors Affecting Surface Wave Propagation*, 4th SEAS DTC Technical Conference, Edinburgh (2009)